PLENARY REPORT

MICRO- AND NANOPOROUS METALS BY SELECTIVE DISSOLUTION OF ALLOYS

Tony Spassov, Lyuben Mihailov, Lyudmila Lyubenova
Faculty of Chemistry and Pharmacy
Sofia University "St. Kliment Ohridski "

Abstract

Micro- and Nanoporous metals have been intensively studied in the recent years. Due to their highly developed surface, good electrical and thermal conductivity and outstanding mechanical stability, they are suitable for various applications in the catalysis, sensing devices, filtering, biotechnology, etc. De-alloying is one of the ways to produce porous materials by selectively dissolving the less noble metal. The other more noble elements undergo reorganization in a three-dimensional nanoporous or microporous structure.

The use of amorphous and nanocrystalline metal alloys as precursors for the production of nanoporous structures by selective dissolution is a new issue, started and developed in our group during the last years. In order to achieve the desired micro- or nanoporous structures, it is necessary to optimize the conditions of electrochemical or chemical dissolution (types and concentrations of electrolyte, temperature, electrode potential). For some of the amorphous alloys etching takes place at a constant rate in three dimensions, which is explained by a surface-controlled dissolution process. The rate of the porous structure formation is very high, as the whole process lasts several minutes. As a result, three dimensional homogeneous micro(nano)porous structures are obtained. In addition, the evolution of morphology and microstructure of nanoporous materials at various stages of bargaining was investigated by SEM and High Resolution Transmission Electron Microscopy (HRTEM) equipped with X-ray microanalysis (EDS). The resulting size of the ligands ranges from tens to hundreds of nanometers. Changes in the composition of the ligaments and microstructure at different dissolution times are associated with the composition of the alloy and the de-alloying mechanism. Furthermore, the microstructure development is associated with the electrocatalytic activity of porous alloys. The electrocatalytic activity with respect to hydrogen and oxygen release of the nanoporous metals is compared with the starting alloys and other known electro-catalytic materials.

Keywords: nanoporous metals, amorphous alloys, de-alloying, selective dissolution.

INTRODUCTION

Porous metals with a high surface-to-volume ratio, low weight, excellent electrical and thermal conductivity are objects of increasing interest in the field of chemistry, mechanics and nanotechnology. Porous nanostructure is ideal for catalysis [1-3], chemical sensors [4, 5] and bio-filtration due to the interconnected nanoporous channels and metal ligaments, which allow easy transport of electrons and medium-sized molecules. A number of approaches have been developed for the production of porous metals, including chemical and electrochemical ones.

De-alloying is one of the methods of obtaining nanoporous materials by selectively dissolving the less noble metal, as the more noble elements rearrange and form the nanoporous structure [6-9]. The size of the pores in the structure depends on the composition of the alloy as well as on the experimental conditions of dealloying (e.g. temperature, type and concentration of the electrolyte, electrochemical potential, etc.).

For the preparation of micro- and nanoporous structures with suitable properties, alloys of different types are used: two-phase crystalline alloys [7,10-15] monophase solid solutions [16-19], nanocrystalline and amorphous alloys [20-22]. To obtain a homogeneous porosity, the system must be monolithic because the elements are reorganized by surface diffusion, and not simply because of the formation of holes after the selective dissolution of one of the phases

of a multiphase system [23].

Lu and co-workers [24] receive copper pore size about 500 nm from a two-phase nanocrystalline Cu62Zr38 alloy by electrochemical dissolution of zirconia in HCl solution. They do not obtain the same result in the selective dissolution of the microcrystalline Cu62Zr38 alloy under the same conditions. Disintegration of the two-phase Cu-20Zr alloy in hydrochloric acid was investigated chemically and electrochemically [25]. The starting alloy is composed of two phases: Cu51Zr14 phase and eutectic Cu-Cu9Zr2. The results show that the dissolution mechanism strongly depends on the electrochemical activity of Zr and Cu in each phase. Nanocrystalline melt-melt Mg-Cu alloys were electrochemically examined in 0.2M aqueous sodium chloride solution [26]. The microstructure obtained after the electrochemical dissolution of Mg60Cu40 is similar to that obtained with the Mg67Cu33 alloy, but the copper nanoparticle size is smaller (about 180 nm).

Sun and colleagues [27] first investigated the formation of a nanoporous nickel film by selectively dissolving the noble element (Cu) from a homogeneous monophase NixCu1-x alloy obtained by electrochemical deposition. The formation of a passive oxide film on the surface of nickel in a sulfamate solution makes it possible to electrochemically etch the copper from the alloy. These results provide general information for the preparation of nanoporous structures by electrochemically selective dissolution of transition metal alloys where the more active component is passivated.

Along with the study of solid solutions of crystalline alloys, it is challenging to use amorphous alloys as precursors for producing porous metals [29]. Compared to crystalline alloys, multi-component metal lenses are monolithic with a homogeneous composition and structure at atomic level. Because of these characteristics, the amorphous alloys are ideal for studying the role of the secondary elements involved in the alloy composition in the selective dissolution. Their surface morphology as well as chemical homogeneity are determinant factors in the selective dissolution process. De-alloying of amorphous Au42Cu29Ti8Si21 and Au44Cu31Ti4Si21 ribbons, resulting in three dimensional ligament structure and micropores have been recently studied[20,28].

The present study includes some of the results and main achievements of our group in Sofia university on the preparation and characterization of micro- and nanoporous metals, using the de-alloying approach. This topic is of wide current interest among the scientific community in the field of Functional materials.

EXPOSITION

Glassy Zr and Cu based alloy ribbons were prepared by rapid quenching from the melt using a melt spinning technique under argon atmosphere. The nanoporous structures were prepared by de-alloying the glassy alloys both chemically and/or electrochemically. SEM (JEOL-5510), TEM (JEOL - 2100, 200 kV) and X-ray diffraction with Cu Kα radiation (Seifert XRD) were used to study the morphology and microstructure of the as-cast and de-alloyed materials. The chemical composition of the as-cast and selectively dissolved alloys was examined by energy dispersive x-ray analysis (EDX). The thermal behavior of the as-cast alloys was studied by differential scanning callorimetry (DSC 7, Perkin-Elmer).

Below we will briefly review some of our more important results on the preparation of micro- and nanoporous metals by de-alloying.

Fig. 1 reveals the X-ray diffraction patterns of ball-milled $Cu_{50}Ag_{50}$ and $Cu_{70}Ag_{30}$ alloys at two different milling times (12 h and 20 h) [17]. For both compositions milling for 12 h leads to alloying and formation of fcc solid solutions. Diffraction peaks of pure Ag and Cu elements can not be detected after 12 h of milling, indicating almost completed alloying process. The diffraction peaks are broad and imply the presence of a nanocrystalline microstructure with average grain sizes of 16 nm for $Cu_{50}Ag_{50}$ and 19 nm for $Cu_{70}Ag_{30}$. It can be concluded that a single-phase supersaturated Cu-Ag solid solutions are formed as a result of the milling. As expected and in agreement with the Vegard's law the fcc solid solution of the alloy with higher Ag content shows larger lattice parameter [17].

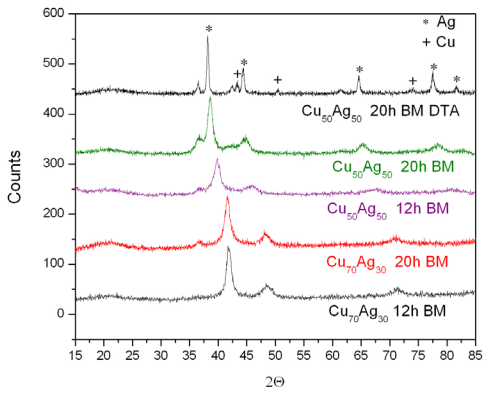

Fig. 1: *X-ray diffraction patterns of ball-milled $Cu_{50}Ag_{50}$ and $Cu_{70}Ag_{30}$ alloys at two different milling times [17]*

The dissolution curves of pure Cu and Ag metals, as well as of $Cu_{70}Ag_{30}$ alloy electrodes are presented in Fig. 2. It is seen that at negative potentials (~ -0.1 V) the current features initially negative values and slowly increases with sweeping the potential in anodic direction. The negative values for the current are due to the oxygen reduction reaction (ORR), which takes place in the entire potential range of interest. It is obvious that the potential, at which the current curve crosses zero (and the Cu dissolution rate clearly takes off in positive direction) is shifted 40 V positively to the dissolution potential of a pure Cu electrode. Taking into account an extrapolation of the alloy curve to an intersection with the potential axis, a quasi-critical potential of dissolution (QCPD) could be identified for the Cu as a less noble component. Thus, the positive potential shift in the alloy dissolution curve is an evidence of single-phase solid solution formation in the immiscible Ag-Cu system, as a result of the ball milling process.

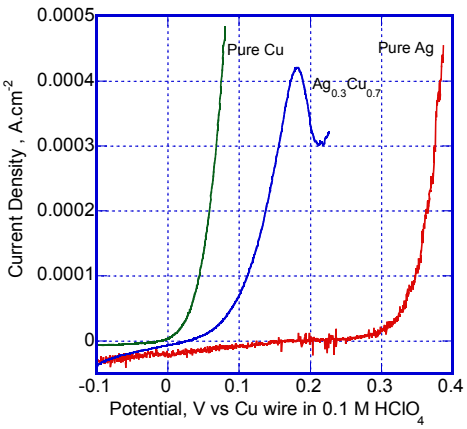

Fig. 2. *Electrochemical dissolution curves, measured at scan rate of 1 mV s^{-1} with pure Cu, Ag, and $Cu_{70}Ag_{30}$ alloy electrodes in 0.1 M $HClO_4$ solution [17]*

The X-ray powder diffraction of the as-cast with two different quenching rates $Zr_{67}Ni_{33}$ alloys (6 and 30 m/s liner velocity of the quenching disc) shows substantial difference in their microstructure, fig. 3 [29]. The alloy quenched with higher velocity is X-ray amorphous and the alloy produced with low cooling rate reveals nanocrystalline microstructure, consisting of about 55 nm tetragonal Zr_2Ni nanocrystals. The mean crystallite size is calculated by the Scherrer equation and is also proved by TEM observations, fig.4. The SAED pattern indicates also that the as-cast with lower velocity alloy is nanocrystalline, containing only tetragonal Zr_2Ni phase.

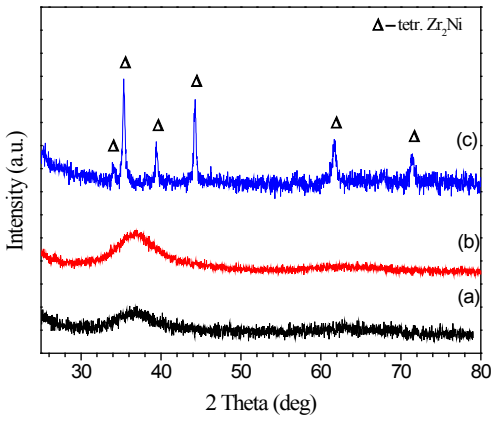

Fig. 3. *X-ray diffraction patterns of Zr67Ni33 quenched with different rates (a – 30 m/s; c – 6 m/s) and of amorphous ribbon (30 m/s) after partial dissolution (curveb) [29]*

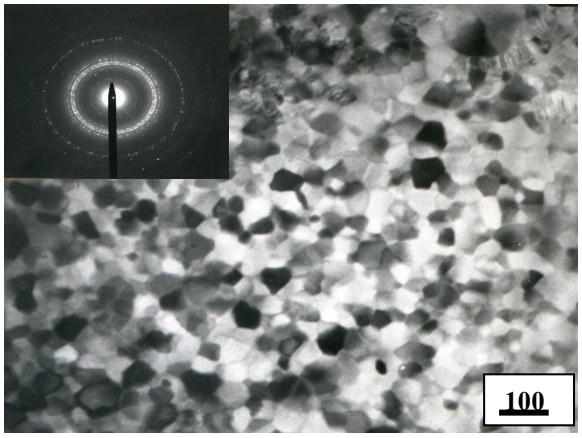

Fig. 4. *TEM and SAED of Zr67Ni33 alloy produced with 6 m/s linear velocity of the quenching disc [29]*

The morphology of the alloys after the potentiostatic experiments at 1100 mV vs. SHE is shown on Fig.5 , clearly indicating a selective dissolution process, which has taken place in both materials. From the SEM micrographs it is evident that the dissolution process in both amorphous and nanocrystalline ribbons starts from certain active centres, which concentration is almost the same for the alloys with different microstructure, N = $2.3x10^4$ cm^{-2}. Once generated the partially dissolved zones start to "grow", forming exact circles in two dimensions (semispheres in three dimensions), which touch each other (overlap) at certain time of selective dissolution. The regular shape of the partially dissolved zones, especially for the amorphous alloy is a clear indication for their three dimensional "growth" with equal rate, i.e. for a partial dissolution process taking place in three dimensions with equal velocity [29].

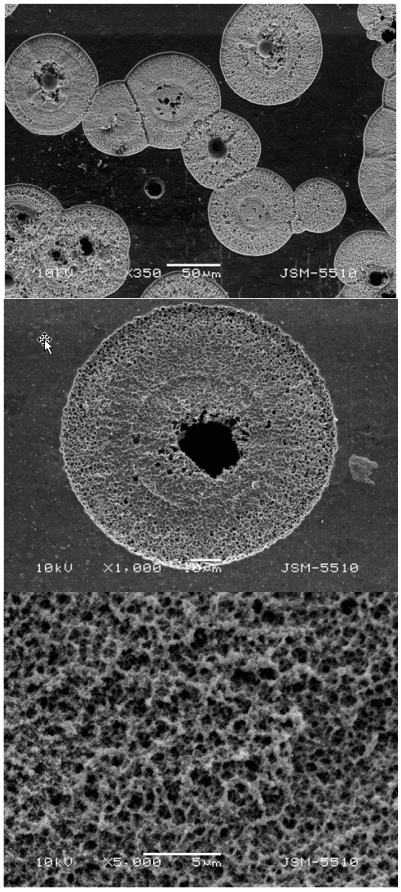

Fig. 5. *SEM micrographs of selectively dissolved amorphous Zr67Ni33 ribbons [29]*

Looking with a higher magnification in a selectively dissolved area (Fig. 5) the average pore size could be determined. Generally, the pores size distribnution is broad for both alloys. Most of the pores of the amorphous alloys are less than 300 nm, but larger pores can also be observed. Generally, the pores in both alloys are relatively large, most probably due to the low diffusion coefficient of the nickel atoms (low atomic mobility of the Ni atoms), which have to rearrange, forming ligaments after removing the Zr atoms in the alloy. The explanation of the observed difference in the pore size of the alloys with different microstructure has to be connected with the mechanism of the dissolution process. While in the amorphous alloys it starts from an active centre, which can be a kind of defect in the otherwise homogeneous disordered structure, and developes uniformly in 3 dimensions, in the nanocrystalline alloys the process most probably starts from the intercrystallite regions and then continues with a predominant selective dissolution of Zr of the smaller crystallites, having larger chemical potential [29].

The de-alloyed samples were studied as electrocatalysts for hydrogen evolution (HER) in 6M KOH. Linear sweep voltammetric measurements were carried out with the amorphous and nanocrystalline alloys before and after selective dissolution, fig. 6. The HE reaction starts at lower potential for the de-alloyed samples, compared to the as-cast alloys, revealing improved activity of the selectively dissolved compared to the as-cast alloys [29].

TEM and selected area electron diffraction confirm that the ribbon is entirely amorphous, fig.7.

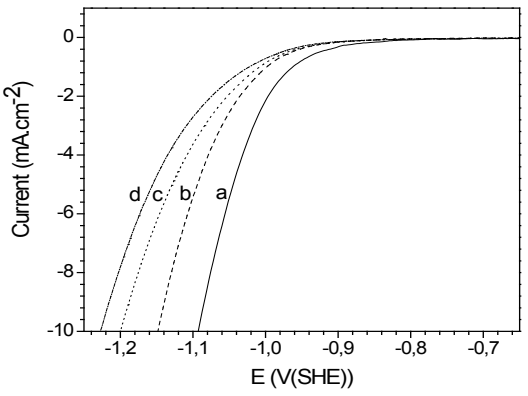

Fig. 6. *Linear sweep voltammetric measurements of amorphous before (d) and after (c) selective dissolution and of nanocrystalline before (b) and after (a) selective dissolution Zr67Ni33 alloys (in 6 M KOH and 25°C) [29]*

Aiming to obtain 3-dimensional microporous metallic structure by selective dissolution and to analyze the influence of the primary alloy microstructure and electrochemical conditions on the morphology and structure of the final porous material (pore and ligament size) amorphous bulk glass forming Zr-based alloys have been studied as well [30]. Based on our previous experience with binary Zr-based glasses Zr-Ni-Cu-Al system was chosen as a precursor for preparing microporous metallic structure first because it is a challenging material for selective dissolution not containing real noble metal and second due to the very good glass forming ability of this system and therefore good opportunity to produce in a maximum degree homogeneous amorphous alloys. The last issue was one of the aims of the study because in general it is not known what kind of heterogeneities into the amorphous material could be the reason to initiate a selective dissolution process either chemically or electrochemically.

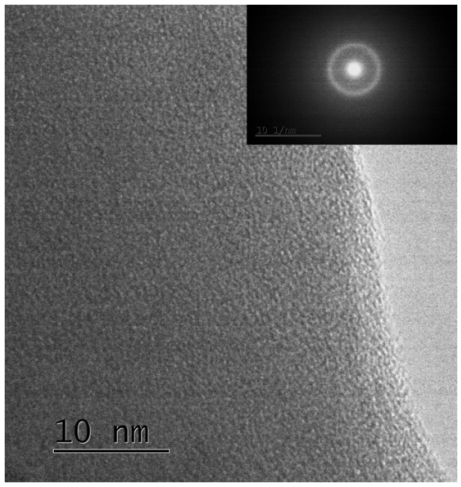

Fig. 7.*TEM micrograph and selected area electron diffraction of as-quenched Zr67.5Cu15Ni10Al7.5 alloy [30]*

Varying the type and the concentration of the electrolyte as well as the electrode potential optimal conditions for selective dissolution of Zr from the Zr-based alloys were obtained. It was found that in the range of potentials 400-1100 mV (vs. SHE) in 0.1M HCl + NaF the process of dissolution is selective, as mainly Zr is leached out together with Al and some Ni. EDAX analysis of the selectively dissolved (dealloyed) zones shows nearly pure Cu in the expense of the other less-noble elements. The time dependence of the corrosion current at different constant potentials (400-1100 mV vs. SHE), selected in the potential range in which Zr is oxydizing, is presented on fig.8. Detailed TEM (electron diffraction) and EDX analyses of the corrosion products show clearly the formation of ZrF_4, Na_3AlF_6 and Na_3ZrF_7. All these compounds are poorly soluble in water and were easily removed with a short time ultrasonic treatment of the dealloyed samples.

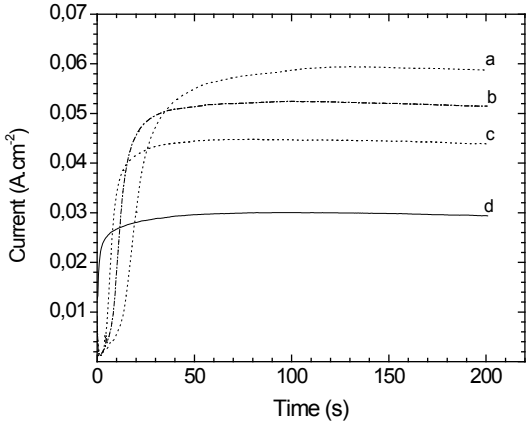

Fig. 8. *Time dependence of the corrosion current at different constant potentials of amorphous Zr67.5Cu15Ni10Al7.5: (a) 1100 mV; (b) 800 mV; (c) 600 mV; and (d) 400 mV (vs. SHE) [30]*

The morphology of the alloys after the potentiostatic selective dissolution at different potentials (400-1100 mV vs. SHE), clearly indicates a selective dissolution process, which has taken place in the studied amorphous metallic ribbons, Figs. 9 and 10, [30]. From the SEM micrographs it is evident that the dissolution process in both as-cast amorphous and relaxed amorphous (annealed at $T_x>T\geq T_g$) ribbon starts from certain active centres, which surface concentration is almost the same for the amorphous alloys, $N = 2.2x10^4$ cm^{-2}. Once generated the partially dissolved zones start to "grow", forming circles in two dimensions (semispheres in three dimensions), which touch each other at certain time of selective dissolution. Although somewhat higher density of the selectively dissolved zones in the areas with some ribbon surface deffects has been observed the overall picture reveals homogeneous distribution of the selectively dissolved regions, as the size of these zones is more or less the same. The last result reveals that during the "growth" of the zones new ones are almost not forming. The rather regular semispherical shape of the partially dissolved zones, especially for the as-cast amorphous alloy, is a clear indication for their three

dimensional "growth" with equal rate. Dividing the radius of the zones by the time of dissolution at certain potential an average "growth" rate of the selectively dissolved zones of about 0.5μm/s was determined. This result entirely confirmed the observations made in our previous study on the selective dissolution of amorphous Zr_2Ni alloys.

Substantial influence of the electrochemical potential on the pores structure and size was not detected, while the influence of the temperature of dissolution was found to be stronger. Considering the initial microstructure of the alloy to be dealloyed it was clearly proved that only the amorphous state (as-cast and relaxed) lead to homogeneous 3-dimensional porous structure, whereas the selective dissolution of the nanocrystalline sample results in the formation of Cu-rich isolated crystalline grains. The surface diffusion coefficient of Cu has also been estimated [30].

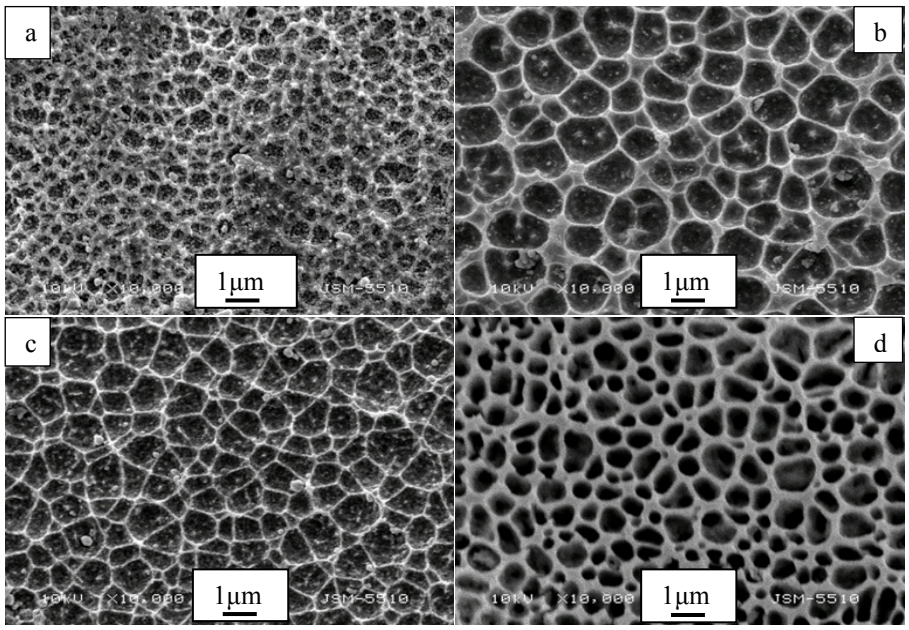

Fig. 9. *SEM micrographs of selectively dissolved Zr67.5Cu15Ni10Al7.5 ribbons at different potentials: (a) 400 mV; (b) 600 mV; (c) 800 mV; and (d) 1100 mV (vs. SHE). Dissolution time – 200 s. [30]*

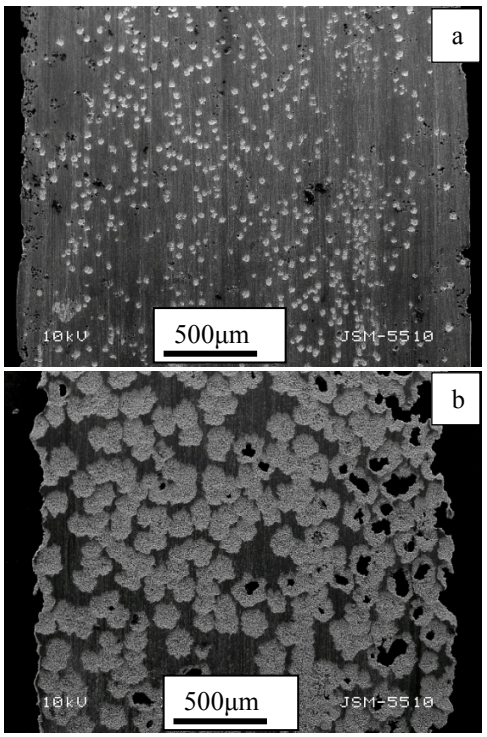

Fig. 10. *SEM micrographs of selectively dissolved Zr67.5Cu15Ni10Al7.5 ribbons at the very beginning (a) and at later stage (b) of the dissolution process at 1100 mV (vs. SHE) [30]*

CONCLUSION

Based on the comprehensive study of the de-alloying of amorphous and nanocrystalline alloys the following main conclusions can be made:

1. Stable nanoporous structures can be prepared by de-alloying of amorphous alloys.
2. De-alloying causes nanocrystallization of the amorphous alloys.
3. Different etching conditions results in different morphology and microstructure of the porous metal (porous structure can be tailored).
4. The electrocatalytic activity in respect to Hydrogen evolution reaction of the amorphous and nanocrystalline alloys after selective dissolution was found to be substantially improved compared to as-cast alloys.
5. Final goal of studying porous metals: combination of good mechanical properties and specific functional properties, leading to practical application.

REFERENCE

[1] J. Snyder, T. Fujita, M. Chen, J. Erlebacher, Oxygen reduction in nanoporous metal–ionic liquid composite electrocatalysts, Nat. Mater. 9 (2010) 904–907.

[2] A. Wittstock, V. Zielasek, J. Biener, C. Friend, M. Bäumer, Nanoporous gold catalysts for selective gas-phase oxidative coupling of methanol at low temperature, Science 327 (2010) 319–322.

[3] J. Zhang, C.M. Li, Nanoporous metals: Fabrication strategies and advanced electrochemical applications in catalysis, sensing and energy systems, Chem. Soc. Rev. 41 (2012) 7016–7031.

[4] Aditya Abburi, Nathan Abrams, Wei Jiang Yeh, Synthesis of nanoporous platinum thin films and application as hydrogen sensor, J. Porous Mater. 19 (2012) 543–549.

[5] R. Shoji, T. Takeuchi, I. Kubo, Atrazine sensor based on molecularly imprinted polymer-modified gold electrode, Anal. Chem. 75 (2003) 4882–4886.

[6] J. Erlebacher, M.J. Aziz, A. Karma, N. Dimitrov, K. Sieradzki, Evolution of nanoporosity in de-alloying, Nature 410 (2001) 450-453.

[7] H.-B. Lu, Y. Li, F.-H. Wang, *Dealloying behavior of Cu–20Zr alloy in hydrochloric acid solution*, Corros. Sci. 48 (2006) 2106–2119.

[8] G. Adamek, J. Jakubowicz, *Microstructure of the mechanically alloyed and electrochemically etched Ti–6Al–4V and Ti–15Zr–4Nb nanocrystalline alloys*, Mater. Chem. Phys. 124 (2010) 1198–1204.

[9] T. Aburada, J.M. Fitz-Gerald, J.R. Scully, *Synthesis of nanoporous copper by dealloying of Al–Cu–Mg amorphous alloys in acidic solution: the effect of nickel*, Corros. Sci. 53 (2011) 1627–1632

[10] S. Brittman, A.J. Smith, S. Milenkovic, A.W. Hassel, *Copper nanowires and silver micropit arrays from the electrochemical treatment of a directionally solidified silver–copper eutectic*, Electrochim. Acta 53 (2007) 324–329.

[11] C. Zhao, X. Wang, Z. Qi, H. Ji, Z. Zhang, *On the electrochemical dealloying of Mg–Cu alloys in a NaCl aqueous solution*, Corros. Sci. 52 (2010) 3962–3972.

[12] H.-Y. Lee, M. Demura, Y. Xu, D.-M. Wee, T. Hirano, *Selective dissolution of the γ phase in a binary Ni(γ)/Ni3Al(γ`) two-phase alloy*, Corros. Sci. 52 (2010) 3820–3825.

[13] S. Milenkovic, V. Dalbert, R. Marinkovic, A.W. Hassel, *Selective matrix dissolution in an Al–Si eutectic*, Corros. Sci. 51 (2009) 1490–1495.

[14] H.-B. Lu, Y. Li, F.-H. Wang, *Synthesis of porous copper from nanocrystalline two-phase Cu–Zr film by dealloying*, Scripta Mater. 56 (2007) 165–168.

[15] R. Mao, S. Liang, X. Wang, Q. Yang, B. Han, *Effect of preparation conditions on morphology and thermal stability of nanoporous copper*, Corros. Sci. 60 (2012) 231–237.

[16] L. Sun, C.-L. Chien, P.C. Searson, *Fabrication of nanoporous nickel by electrochemical dealloying*, Chem. Mater. 16 (2004) 3125–3129.

[17] T. Spassov, L. Lyubenova, Y. Liu, S. Bliznakov, M. Spassova, N. Dimitrov, *Mechanochemical synthesis, thermal stability and selective electrochemical dissolution of Cu–Ag solid solutions,* J. Alloys Compd. 478 (2009) 232–236.

[18] X. Lu, E. Bischoff, R. Spolenak, T.J. Balk, *Investigation of dealloying in Au–Ag thin films by quantitative electron probe microanalysis*, Scripta Mater. 56 (2007) 557–560.

[19] J.-K. Chang, S.-H. Hsu, I.-W. Sun, W.-T. Tsai, *Formation of nanoporous nickel by selective anodic etching of the nobler copper component from electrodeposited nickel–copper alloys*, J. Phys. Chem. C 112 (2008) 1371–1376.

[20] F. Scaglione, A. Gebert, L. Battezzati, *Dealloying of an Au-based amorphous alloy*, Intermetallics 18 (2010) 2338–2342.
[21] X.Y. Lang, H. Guo, L.Y. Chen, A. Kudo, J.S. Yu, W. Zhang, A. Inoue, M.W. Chen, *Novel nanoporous Au–Pd Alloy with high catalytic activity and excellent electrochemical stability*, J. Phys. Chem. C 114 (2010) 2600–2603.
[22] T. Aburada, J.M. Fitz-Gerald, J.R. Scully, *Synthesis of nanoporous copper by dealloying of Al–Cu–Mg amorphous alloys in acidic solution: the effect of nickel*, Corros. Sci. 53 (2011) 1627–1632.
[23] J. Yu, Y. Ding, C. Xu, A. Inoue, T. Sakurai, M. Chen, *Nanoporous metals by dealloying multicomponent metallic glasses*, Chem. Mater. 20 (2008) 4548–4550.
[24] H.-B. Lu, Y. Li, F.-H. Wang, *Synthesis of porous copper from nanocrystalline two-phase Cu–Zr film by dealloying, Scripta Mater. 56 (2007) 165–168.*
[25] H.-B. Lu, Y. Li, F.-H. Wang, *Dealloying behavior of Cu–20Zr alloy in hydrochloric acid solution*, Corros. Sci. 48 (2006) 2106–2119.
[26] C. Zhao, X. Wang, Z. Qi, H. Ji, Z. Zhang, *On the electrochemical dealloying of Mg–Cu alloys in a NaCl aqueous solution*, Corros. Sci. 52 (2010) 3962–3972.
[27] L. Sun, C.-L. Chien, P.C. Searson, *Fabrication of nanoporous nickel by electrochemical dealloying*, Chem. Mater. 16 (2004) 3125–3129.
[28] E.M. Paschalidou, F. Celegato, F. Scaglione, P. Rizzi, L. Battezzati, A. Gebert, S. Oswald, U. Wolff, L. Mihaylov, T. Spassov, The mechanism of generating nanoporous Au by de-alloying amorphous alloys, *Acta Materialia* 119 (2016) 177-183.
[29] L. Mihailov, Murad Redzheb, T. Spassov, *Selective dissolution of amorphous and nanocrystalline Zr_2Ni*, Corrosion Science 74 (2013) 308–313.
[30] L. Mihaylov, L. Lyubenova, Ts. Gerdjikov, D. Nihtianova, T. Spassov, Selective dissolution of amorphous Zr-Cu-Ni-Al alloys, *Corrosion Science* 94 (2015) 350–358; doi:10.1016/j.corsci.2015.02.031.